GSA DATA REPOSITORY 2014348

Supplementary materials for
Seasonal, long-term, and short-term deformation in the Central Range of Taiwan induced by landslides

Ya-Ju Hsu[1], Rou-Fei Chen[2], Ching-Weei Lin[3], Horng-Yue Chen[1], Shui-Beih Yu[1]
1. Institute of Earth Sciences, Academia Sinica, Taipei, Taiwan
2. Department of Geology, Chinese Culture University, Taipei, Taiwan
3. Department of Earth Sciences, National Cheng Kung University, Tainan, Taiwan

1. GPS position time series at sites affected by landslides

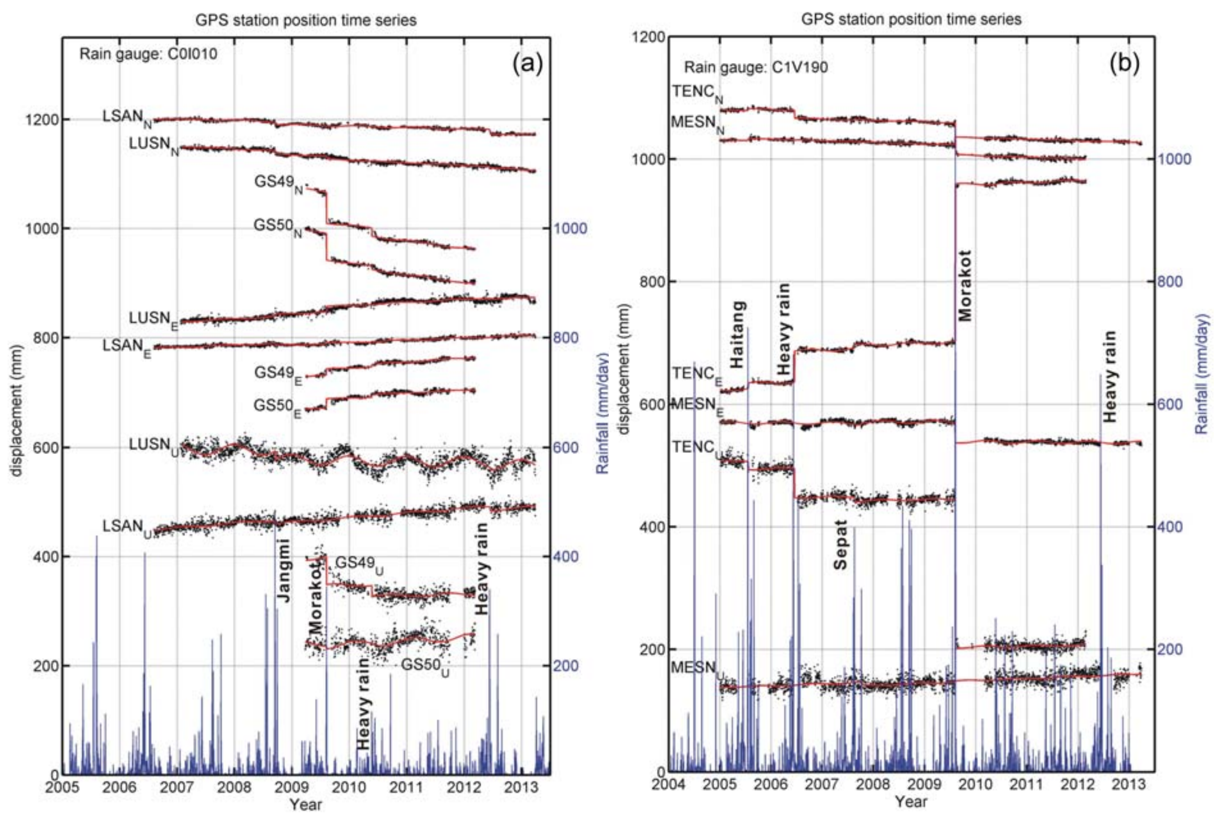

Figure DR1. Black dots denote GPS position time series after removing interseismic velocities and offsets due to instrument changes. Red lines indicate modeled time series. Blue lines show daily rainfall. Rainfall events or typhoons caused significant surface displacements are shown as black texts. Locations of sites are shown in Figure 1A.

2. The time and durations of heavy rains and typhoons in this study

Table DR1. Time and durations of heavy rains and typhoons in the study period

Event	Date	Day of year
2005 Haitang	2005/07/16-2005/07/20	197-201
2006 Heavy rain	2006/06/05-2006/06/12	156-163
2007 Sepat	2007/08/16-2007/08/19	228-231
2007 Krosa	2007/10/04-2007/10/07	277-280
2008 Jangmi	2008/09/26-2008/09/29	270-273
2009 Morakot	2009/08/05-2009/08/10	217-222
2010 Heave rain	2010/05/21-2010/05/24	141-144
2012 Heave rain	2012/06/08-2012/06/12	160-164

3. Interpolated interseismic vertical velocities

The interseismic uplift rates in the Lushan area are the largest in central Taiwan (inset on bottom right of Figure 1A); while the cGPS sites here are affected by landslides and not used for interpolation of interseismic velocity field. The interpolated interseismic vertical velocities (Figure DR2) at sites in Lushan are likely to be underestimated, resulting in estimates of long-term uplift due to landslides.

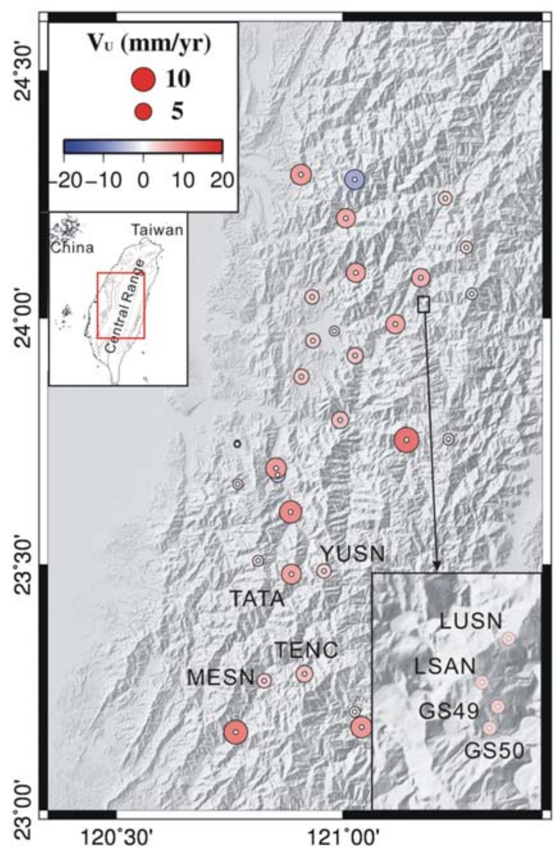

Figure DR2. Interseismic GPS vertical velocities in the Central Range of Taiwan. Vertical rates at sites affected by landslides (station name are shown) are interpolated from the adjacent stable cGPS sites.

4. **Topography and time series of station position at TENC**

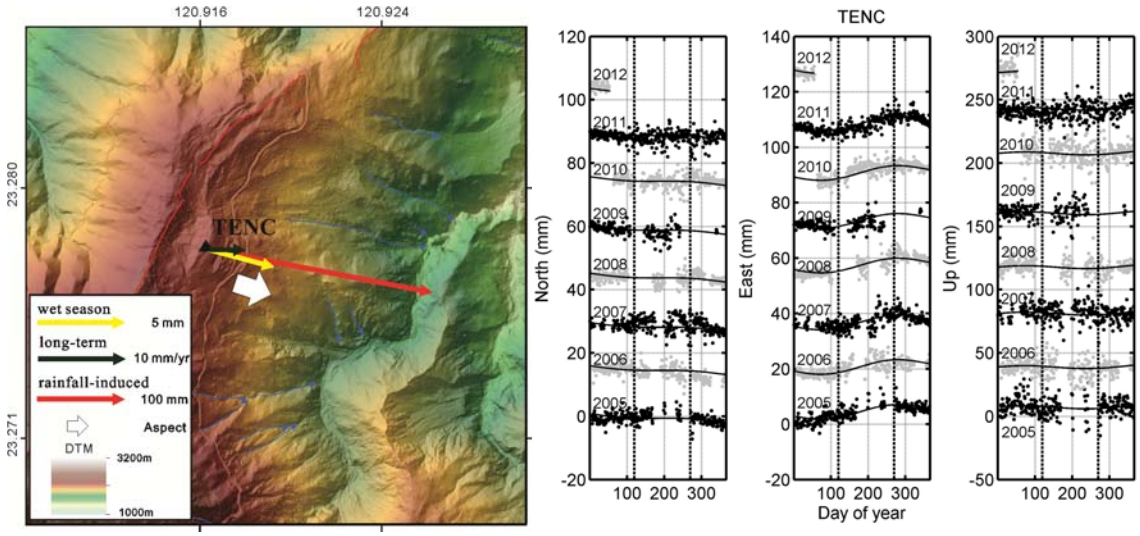

(a) (b)

Figure DR3. (a) Topography derived from LiDAR (1 m × 1 m). Red and blue lines indicate fault scarps and gullies, respectively. Red vectors indicate GPS displacements of the largest rainfall-induced landslide from 2005 to 2013 (Table DR3). Black and yellow vectors indicate landslide-induced long-term linear rates and additional motions in the wet season, respectively. White vector denotes aspect of slope derived from LiDAR. (b) GPS time series of north, earth, and vertical components. We add a constant offset and switch color between black and gray every year for better visualization. Solid line is the model with a landslide-induced long-term linear rate and periodic annual motions.

5. Landslide-induced long-term secular motion, motions in the wet season and during the largest rainfall-driven landslides from 2005 to 2013

Landslide induced long-term linear rates are estimated from the differences between original long-term linear velocities at unstable sites (blue vectors in Figure 1A) and the interpolated interseismic velocities (black vectors).

Table DR2. Rates and directions of landslide-induced long-term secular motions and additional GPS motions in the wet season. Slope and aspect of each hillslope are derived from LiDAR.

	Landslide-induced long-term motion					Additional motion in the wet season					LiDAR	
	V_E (mm/yr)	V_N	V_U	V_H	Azi (°)	dE (mm)	dN	dU	dH	Azi (°)	Slope (°)	Aspect (°)
GS49	6.9	-13.5	2.1	15.1	153	2.2	-3	-5.6	3.7	144	25	163
GS50	4.8	-14.4	6.9	15.2	161	1.4	-2	11.2	2.4	145	12	163
LUSN	5.8	-5.0	-1.2	7.7	131	2	-1	-18.8	2.2	117	30	132
LSAN	4.5	-2.4	8.5	5.1	118	2.2	-2.6	-3.2	3.4	140	32	163
YUSN	-6.2	-2.6	-8.3	6.7	247	-1.2	2	-4	2.3	335	40	225
TATA	-12.4	5.6	-0.3	13.6	294	-5.0	4.6	-1.8	6.8	313	38	306
TENC	4.1	-0.1	2.5	4.1	91	3.8	-1	-3	3.9	105	35	108
MESN	2.4	-2.2	-0.5	3.3	131	-4.4	-0.8	2.6	4.5	260	12	265

Table DR3. GPS surface displacements of the largest rainfall-induced landslides from 2005 to 2013. Slope and aspect of each hillslope are derived from LiDAR.

		Displacements of the largest rainfall-induced landslide						LiDAR	
	Event	dE (mm)	dN (mm)	dU (mm)	dH (mm)	Azi (°)	Plunge (°)	Slope (°)	Aspect (°)
GS49	2009 Morakot	9.7	-56.4	-49.8	57.2	170	41	25	163
GS50	2009 Morakot	16.0	-48.6	5.2	51.2	162	6	12	163
LUSN	2008 Jangmi	3.8	-6.0	-16.8	7.1	148	67	30	132
LSAN	2012 heavy rain	0.2	-7.2	-7.4	7.2	178	46	32	163
YUSN	2009 Morakot	-41.9	-6.2	-41.8	42.4	262	45	40	225
TATA	2009 Morakot	-46.8	20.9	-28.1	51.3	294	29	38	306
TENC	2009 Morakot	256.9	-51.7	-241.9	262.1	101	43	35	108
MESN	2009 Morakot	-33.0	-12.2	3.4	35.2	250	6	12	265

6. Rainfall-induced landslides at site TENC during the 2009 Typhoon Morakot

The TENC site started to move when the amount of cumulative rainfall increase to 1000 mm and then the motion was accelerated when the cumulative rainfall was up to 2000 mm and slowed down two days later after rain stopped.

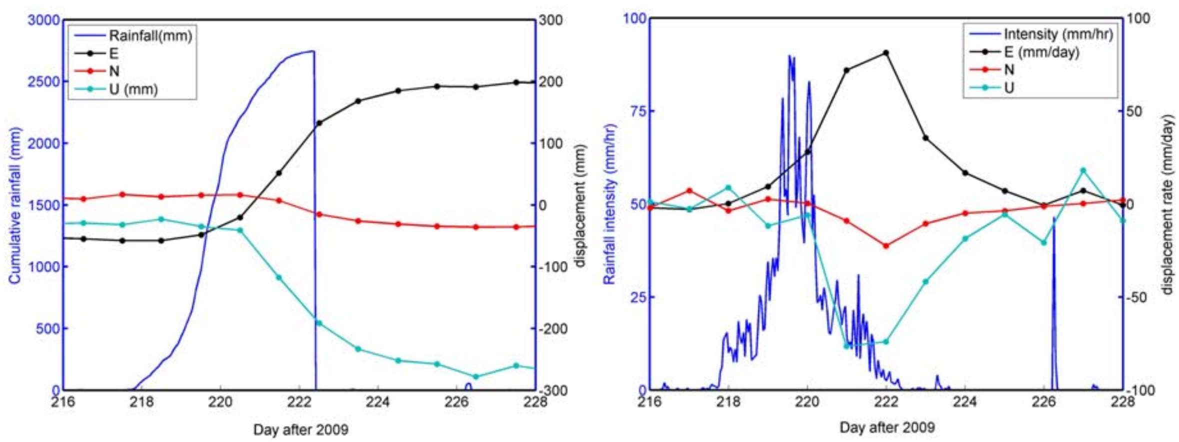

(a) (b)

Figure DR4. Relations between the rainfall and GPS displacements during the 2009 Typhoon Morakot. (a) Blue curve denotes cumulative rainfall during Typhoon Morakot. Black, red, and light blue curves indicate GPS position time series of east, north and vertical components, respectively. (b) Blue curve denotes rainfall intensity (mm/hr) during the Typhoon Morakot. Black, red, and light blue curves indicate GPS displacement rates of east, north and vertical components, respectively.

7. Relations between seismic activity and landslides

Locations of landslides discovered in this study are correlated neither with the earthquake density, nor with the cumulative seismic moment. This observation is consistent with rainfall-driven landslides. More detailed information about earthquake-triggered landslides can be found at Meunier et al. (2008).

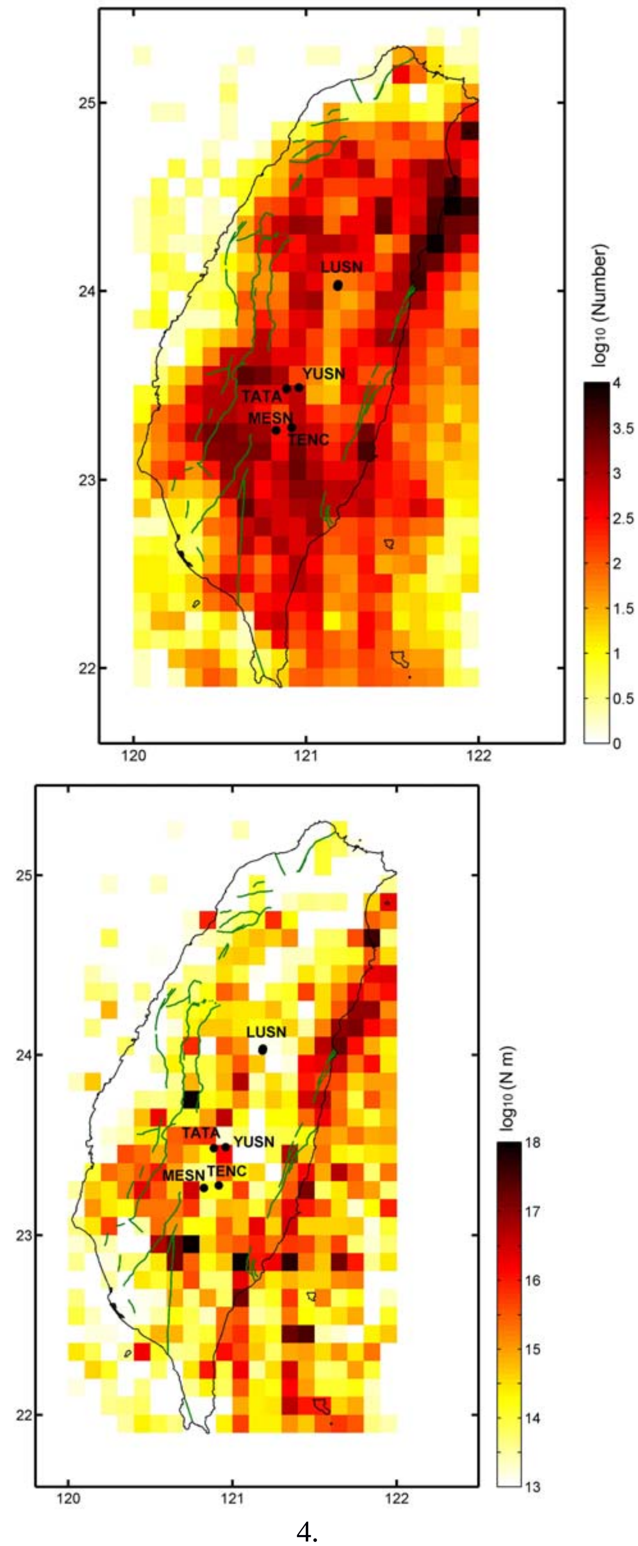

4. (b)

Figure DR5. Spatial distributions of earthquake density and seismic moment from 2005 to 2012. (a) Color scale indicates earthquake density at each 0.1°×0.1° gird cell. The seismic catalog is obtained from the Central Weather Bureau of Taiwan. Green lines show major faults. Black dots denote GPS sites affected by landslides. (b) Color scale indicates cumulative seismic moment from 2005 to 2012 at each 0.1°×0.1° gird cell

8. Relations between the amplitude of surface displacements, the maximum rainfall intensity, and the cumulative rainfall at each event

We plot landslides events in the study period from 2005 to 2013. Time and durations of heavy rains or typhoons at each event are shown in Table DR1.

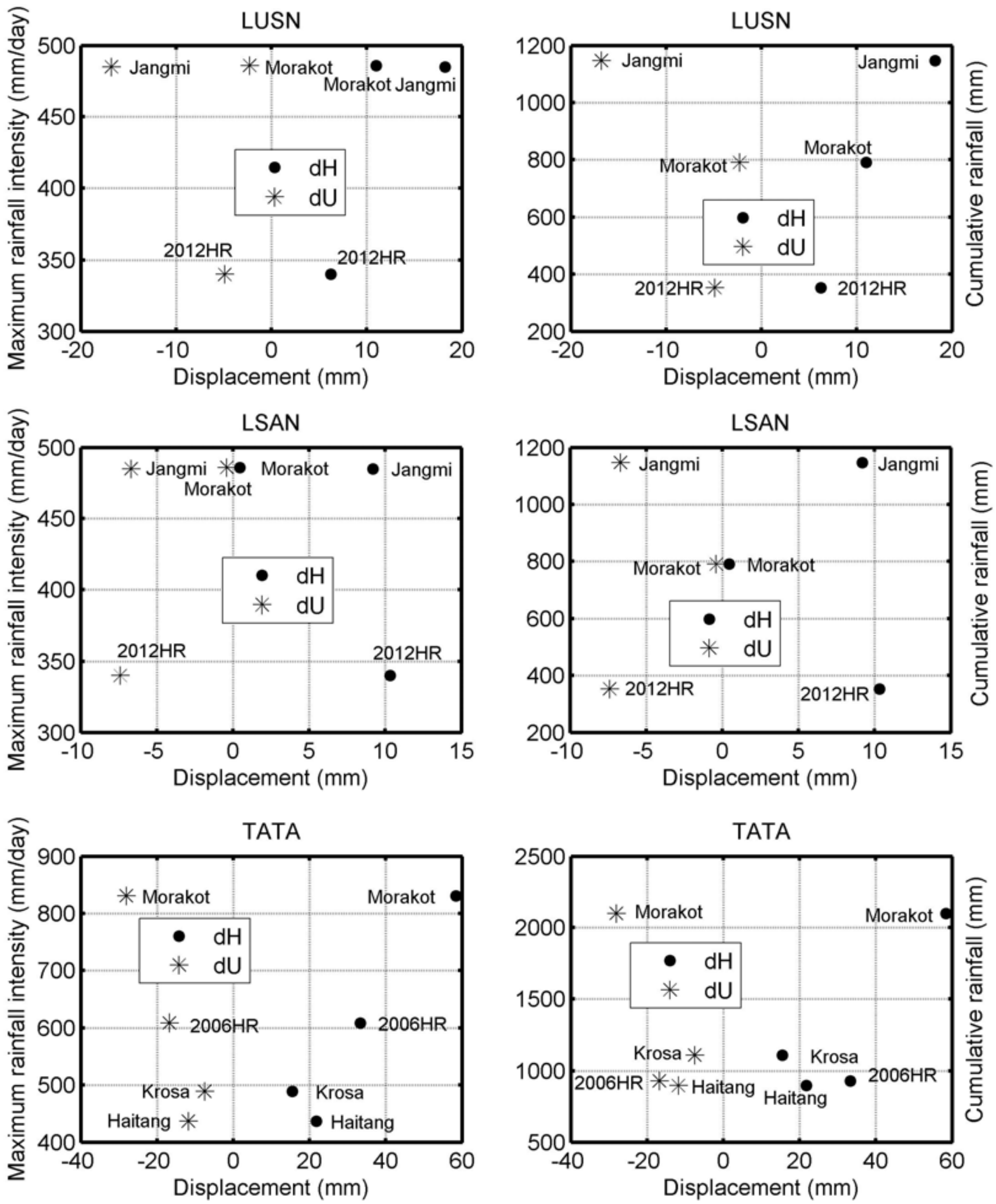

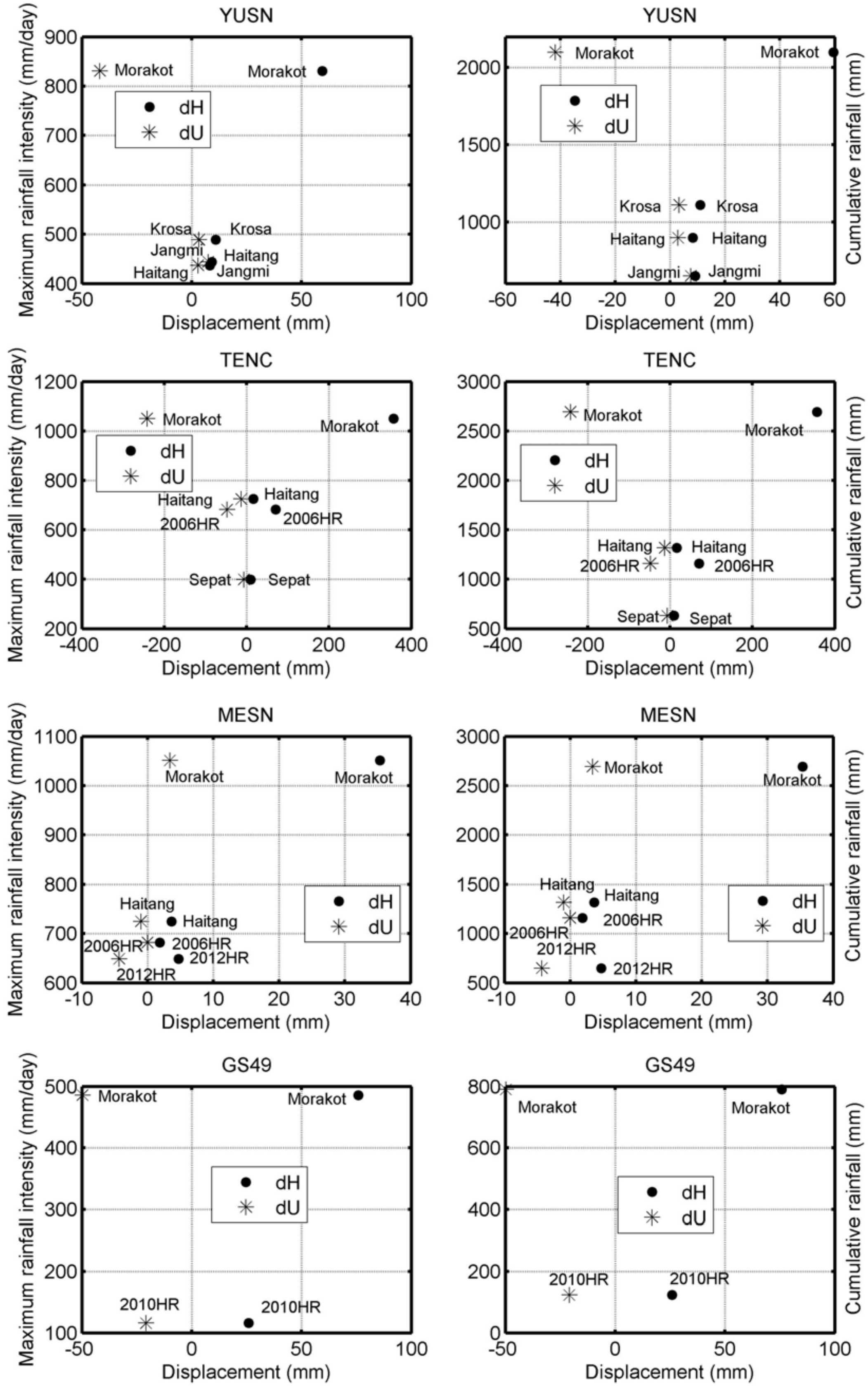
YUSN
Maximum rainfall intensity (mm/day)
Displacement (mm)
Morakot
Krosa
Jangmi
Haitang
dH
dU
YUSN
Cumulative rainfall (mm)
Displacement (mm)
Morakot
Krosa
Haitang
Jangmi
TENC
Maximum rainfall intensity (mm/day)
Displacement (mm)
Morakot
Haitang
2006HR
Sepat
TENC
Cumulative rainfall (mm)
Displacement (mm)
Morakot
Haitang
2006HR
Sepat
MESN
Maximum rainfall intensity (mm/day)
Displacement (mm)
Morakot
Haitang
2006HR
2012HR
MESN
Cumulative rainfall (mm)
Displacement (mm)
Morakot
Haitang
2006HR
2012HR
GS49
Maximum rainfall intensity (mm/day)
Displacement (mm)
Morakot
2010HR
GS49
Cumulative rainfall (mm)
Displacement (mm)
Morakot
2010HR

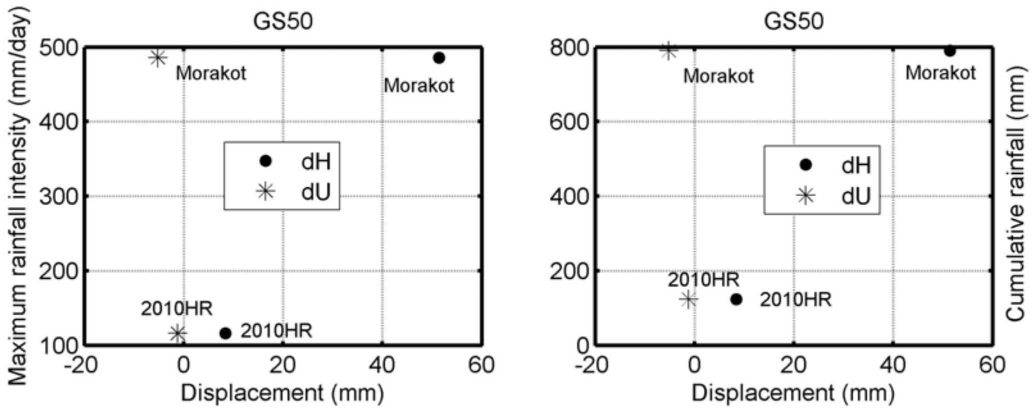

Figure DR6. Left and right panels show the relationships between the maximum rainfall intensity and GPS displacements at each event and between the cumulative rainfall and GPS displacements at each event, respectively. “dH” and “dU” denote GPS horizontal and vertical displacements associated with landslides. “HR” represents for Heavy Rain.

References

Chen C.-H., H.-C. Ho, K.-S. Shea, W. Lo, W.-H. Lin, H.-C., Cheng, C.-S. Huang, C.-W. Lin, G.-H. Chen, C.-N. Yang and Y.-H. Lee, 2000, Geologic map of Taiwan, Central Geological Survey, Ministry of Economic Affairs.

Meunier, P., Hovius, N., and Haines, J. A., 2008, Topographic site effects and the location of earthquake induced landslides: Earth and Planetary Science Letters, v. 275, no. 3-4, p. 221-232.